Transport and Communications Science Journal

INFLUENCE OF FINE AGGREGATES REPLACED RATIO ON SHEAR STRENGTH OF OYSTER SHELL CONCRETE BEAM USING GFRP REBARS

Tu Sy Quan

University of Transport and Communications, No 3 Cau Giay Street, Hanoi, Vietnam

ARTICLE INFO

TYPE: Research Article
Received: 05/06/2024
Revised: 07/09/2024
Accepted: 12/09/2024
Published online: 15/09/2024
https://doi.org/10.47869/tcsj.75.7.11

* *Corresponding author*
Email: tusyquan@utc.edu.vn; Tel: +84973767555

Abstract. The recycle of oyster shell as a component of concrete is a considerable solution around the world, not only ameliorate environment quality due to waste pollution but also decelerate the depletion of traditional aggregates. In this study, the oyster concrete is elaborated and performed in the order to determine many mechanic properties such as compressive strength, tensile strength or modulus of elasticity. These parameters are an important information, allowing to predict the shear strength of concrete in the structure using Glass Fiber Reinforced Polymer (GFRP) rebar, where a part of fine aggregate is replaced by oyster shell. Besides, many 3-points bending test were realized in several beams with different ratios of replacement. The presence of oyster shell crushed replacing the natural sand reduced many mechanic characteristics of concrete, including the shear behaviour. However, compared to theoretical predictions, the results given by experiment seems betters, although there is a diminution of shear strength in almost specimens. This argument leads to the possibility of using this kind of concrete with GFRP rebar in the design of manufacturing precast members, mainly under the load introducing the shear force.

Keywords: oyster shell concrete, GFRP rebar, shear strength, 3-point bending test, seashell concrete.

1. INTRODUCTION

Quang Ninh is a famous province considering the area and production of oyster farming. In addition, there are also a few localities in the South and Central South region that raise oysters on a lower scale such as Ninh Thuan, Can Gio, Khanh Hoa but the oyster meat is taken as food for lobster rafts or sea fish, according to statistic from Vietnam Fisheries Magazine [1]. The death massively of oysters causes many farming households not only to

lose hundreds of billions VND, but also creates additional impacts for waste treatment, causing environmental pollution. Also, according to the report of Gia Dinh Vietnam newspaper [2], the oyster processing factory of Ha Long Production Development Investment Company Limited (Bim Group), located in Dong Hai village, Dong Xa commune, Van Don district, Quang Ninh province, whose main activities are oyster pre-processing and processing, has been received the problems with the waste treatment. Besides discharging the wastewater, the seashells treatment is also a problematic issue for this factory. A part of the oyster shell after being extracted will be reused for seeding and the rest will be rejected. Against the large production like this factory, the oyster shell waste collecting is not simple. The smell arising from the oyster shell collection area has not been paid attention to eliminate. The discomfort of pollution makes local peoples worried and unsecured. Otherwise, the increasing demand for construction domain leads to finding the new friendly kind of aggregates. In this perspective, Steven D. Palkovic et al.(2016) [3] conducted a comparison of four materials, potentially replaced for cement concrete in structures, including bone, deep sponge, seashell and cement concrete at macro, meso, micro and nano scale. The results shown that, at the meso scale, seashells are composed by layers of Aragonite leaves, a mineral of carbonate origin $CaCO_3$, suitable to replace the traditional aggregates. Many studies summed up by Morris (2017) [4], have shown that seashells can be used as a substitute part for both cement and aggregates in concrete. Its applications existing for a long time, can be schematized in Figure 1. Heating the peels at high temperatures and grinding to achieve the appropriate fineness are desirable processing methods that improve product quality. Although workability, compressive strength, tensile strength and elastic modulus are reduced, seashell waste can still be used as aggregate at partial replacement levels, up to 50% for sufficient providing the workability and strength of concrete for non-structural and structural purposes [5,6].

Figure 1. Example of oyster concrete and its applications [4].

From experimental results, Monita Olivia et al. [7] also concluded that using seashells to replace traditional aggregates significantly improves the tensile and flexural strength of concrete, while the compressive strength and modulus of elasticity are depending on aggregate size. Consequently, the reusing waste oyster shells as construction aggregate is an urgent and useful topic, not only helps to increase the economic value of oyster shells, thereby limiting risks for farmers but also solve the difficulty from environmental problematic of the exploiting process and seafood processing.

2. PREDICTING THE SHEAR STRENGTH OF FLEXURAL MEMBER IN PRESENT CODES

Against reinforced concrete structures, theoretical models in shear strength provision are often classified on two main groups: Strut and tie model – STM and Modified Compression Field Theory-MCFT. According to review of Imad Shakir [8], the general design procedures using the STM model for reinforced concrete structures are addressed by various codes of practices such as ACI 318, CSA S806, CSA S6, Eurocode 2, etc.

Table 1. Shear calculation method for concrete beams reinforced with FRP bars.

Specifications	Shear strength of concrete	Shear strength of GFRP rebar
ACI 440.1R-15	$V_c = \left(\frac{12}{5}k\right)0.167\sqrt{f_c'}b_w d$	$V_f = \frac{A_f f_{fv} d}{s}$
JSCE 1997	$V_{cf} = \beta_d \beta_p 0.2\sqrt[3]{f_c'}b_w d$	$V_{sf} = \frac{A_{fw} E_{fw} \varepsilon_{fwd}}{s} z$
CSA S806-12	$V_c = 0,05\lambda\phi_c k_m k_r k_a k_s \left(f_c'\right)^{1/3} b_w d_v$	$V_{sf} = \frac{\phi_f A_{fv} f_{fv} d_v}{s}\cot\theta$
BS-8110	Case 1: $\frac{a}{d} < 2.5$ $V_c = \frac{0,79}{\gamma_{me}}\left(\frac{100.A_{ref}}{b_w d_v}\frac{f_c'}{25}\right)^{1/3}\left(\frac{400}{d}\right)^{1/4} b_w d_v \left(2\frac{d_v}{a}\right)$ Case 2: $\frac{a}{d} > 2.5$ $V_c = \frac{0,79}{\gamma_{me}}\left(\frac{100.A_{ref}}{b_w d_v}\frac{f_c'}{25}\right)^{1/3}\left(\frac{400}{d}\right)^{1/4} b_w d_v$	$V_{sf} = \frac{0.0025 E_{fw} A_{fw}}{\gamma_{me}}\frac{d}{s}$

Meanwhile, the modified compression field theory (MCFT) described by Vecchio et al [9] is a general model for the load-deformation behaviour of two-dimensional cracked reinforced concrete subjected to shear. This theory has also been officially used in AASHTO LRFD for shear design of reinforced concrete structures. In this study, the calculations from four specifications related to shear performance prediction were practiced, such as ACI 440.1R-15, JSCE 1997, CSA S806-12, BS-8110 [10-13]. The formula using for this research can be recapitulated in Table 1 and the main contents of these specifications are reported in Annex of this article.

3. DETERMINING MATERIAL PROPERTIES

The scientific name of seashell selected for this study is Pacific Oyster, exploited from Van Don, Quang Ninh. They are dried, crushed and sieved at 4,75mm before the elaboration of specimens. The components are the same for three mixture excepting the fine aggregates. A partial natural sand will be replaced by oyster crushed, respectively 0%, 25% and 50%. The mixture components in oyster shell concrete were mixed for a total of 8 minutes. Song Da sand, crushed oyster shells and binder ingredients such as But Son cement and fly ash are mixed dry within 2 minutes. After that, add 70% of the water and continue mixing for 2 minutes. Finally, add the superplasticizer to 30% remaining water, add it to the concrete mixture and mix for 4 minutes to finish the mixing process. The composition of concrete

mixture is selected according to guidelines of ACI 211.4R-08 [14], can be exhibited as following table 2:

Table 2. Design composition for one cubic meter of concrete mixtures.

Components	Units	OSCB-S-0	OSCB-S-25	OSCB-S-50
PC40 cement	kg	454.5	454.5	454.5
Natural sand dried	kg	635.7	476.8	317.8
Gravel 5x10 dried	kg	1040	1040	1040
Oyster shells dried	kg	0	63.1	126.2
Water	liter	208.9	213.5	218.0
Fly ash (F)	kg	80.2	80.2	80.2
Admixture	liter	5.6	5.6	5.6

The slump test was determined in parallel with the moulding process, shown in Figure 2. The cylindrical specimens were manufactured with dimensions of 150x300 mm in accordance with the specifications ASTM C39 [15] and ASTM C469 [16] serving the test to determine compressive strength at different days of age and elastic modulus at 28 days of age.

Figure 2. Elaboration process of specimens.

In addition, 4-point bending tests on 12 rectangular specimens with dimensions of 100x100x400 mm allowing to determine the tensile flexural strength. The experimental steps respected to guidelines of ASTM C78-02 [17]. The experimental work to determine the technical properties of oyster shell concrete is shown in Figure 3 and the test results are summarized in the Table 3:

Table 3. Mechanic properties of three concrete mixtures.

Categories	OSCB-S-0	OSCB-S-25	OSCB-S-50
Compressive strength (MPa)	56.8	42.3	37.2
Tensile Flexural strength (MPa)	8.6	6.3	4.9
Elastic modulus (MPa)	33764	24643	23517

a) Compresive strength test b) Modulus of elasticity test c) Tensile flexural strength test

Figure 3. Perspective of test operations determining the mechanic proprieties of oyster concrete.

4. EXPRIMENTAL PROTOCOL

4.1. Design of reinforcement

The beam specimens are manufactured with the same geometric dimensions and the same GFRP reinforcement arrangement. The beams are designed and the GFRP reinforcement content is selected so that the failure mode occurs on the concrete before the GFRP reinforcement is broken.

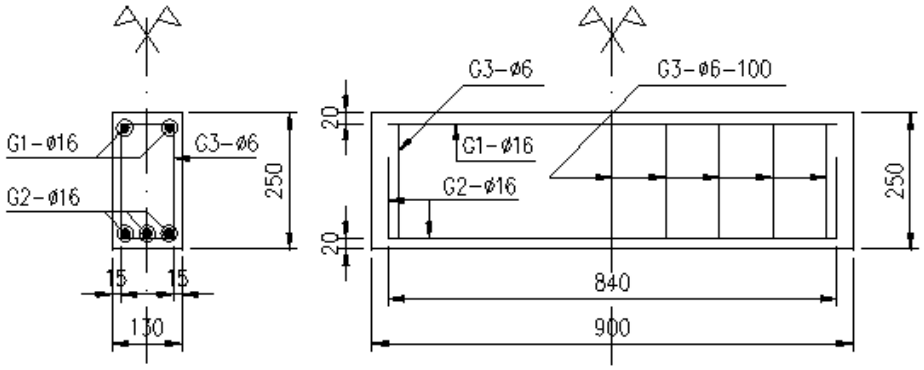

Figure 4. Dimensions of beam specimens and arrangenent of GFRP reinforcement.

In particular, three beam specimens have a length of 900mm, cross section 130×250mm corresponding to three concrete mix components, respectively 0%, 25% and 50% volume of sand replaced by crushed oyster shells. Especially, the characteristics of the beam specimen reinforcement in the study is captured in the Table 3. Compared to elastic modulus of non prestressed steel, always taken equal to 200GPa, according to ACI 318-14 [18], GFRP material provide the smaller stiffness. The GFRP rebars with elastic modulus of 45GPa and ultimate tensile strength of 800MPa were selected for these beams reinforcing.

Table 4. Specifications of beam reinforcement details.

Categories	OSCB-S-0	OSCB-S-25	OSCB-S-50
Top longitudinal reinforcement (G1)	2Ø16	2Ø16	2Ø16
Bottom longitudinal reinforcement (G2)	3Ø16	3Ø16	3Ø16
Stirrup (G3) (a haft of span)	Ø6@100	Ø6@100	Ø6@100

4.2. Creation and curing procedure

After the geometric treatment in the factory, GFRP reinforcement are installed according to the design such as the correct quantity, dimension and distance between us by using tie wire. On each beam, there are strain gauges glued to measure the deformation of longitudinal reinforcement and stirrup.

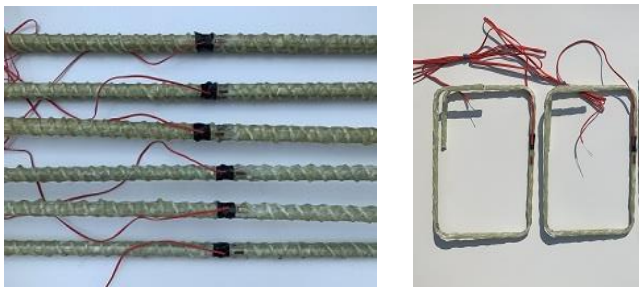

Figure 5. Strain gauges are glued on the face of GFRP reinforcement.

Besides, the formwork is elaborated from steel, installed and cleaned before applying a layer of non-stick oil. The GFRP frame is then placed into the mould and its position is fixed to two ends of the mould by tie wire. The formwork system is horizontally placed at a flat position. To ensure the imperviousness of formwork during the concrete pouring process, many open areas are sealed by silicon. The concrete component is mixed respecting to the design mixture, each batch is tested for slump and temperature in order to ensure the workability of the concrete. To ensure consistency, concrete is poured layers by layers and compacted by using Ø16 steel rods and rubber hammers. The concrete pouring process is finished with the surface of the test specimens. The process is described in Figure 6. After 4 hours of casting the specimens, the top surface of the specimens will be covered with moist sand and sprayed regularly every 3 hours, ensuring the specimens and sand are always in humid state, as shown in Figure 7.

Figure 6. Compacting and pouring concrete process.

Figure 7. Curing beam specimens after casting with moist sand.

The mold removal process takes no less than 3 days for each specimen. The beam specimens were checked for geometric and surface dimensions to ensure that the beams were manufactured according to design and that no cracks appeared before conducting the experiment. After that, the beams were cured at temperature 22°C in the laboratory condition.

4.3. Test set up and measurement

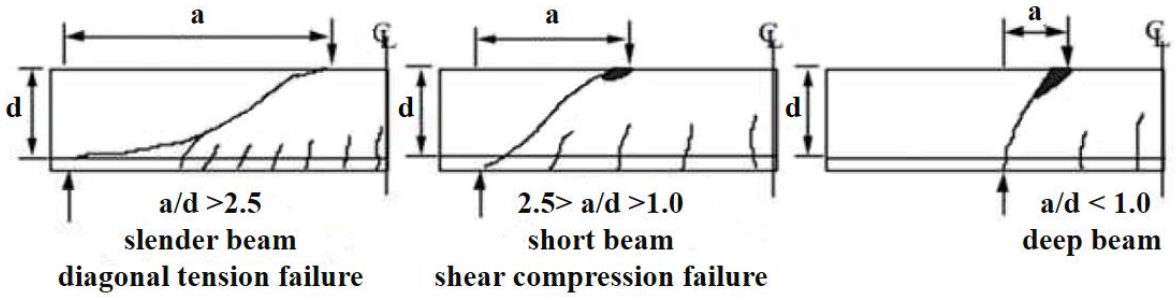

Figure 8. Typical forms of failure on traditional reinforced concrete beams according to review of U.Farooq et al [19].

Against traditional reinforced concrete structures, many studies have shown that the ratio of shear span to beam height (a / d) has an effect on the formation, distribution of cracks and failure state, specifically as follows:

- Damage due to purely shear: $a / d < 1$
- Damage due to shear-compression: $1 < a / d < 2,5$
- Damage due to diagonal tension: $2,5 < a / d < 6$

Figure 8 illustrates the above failure forms corresponding to the formation and distribution of cracks in each case.

The specimens in this study, were tested according to the 3-point bending principle with the applying force at the middle and two supporting pins on both sides as in Figure 9.

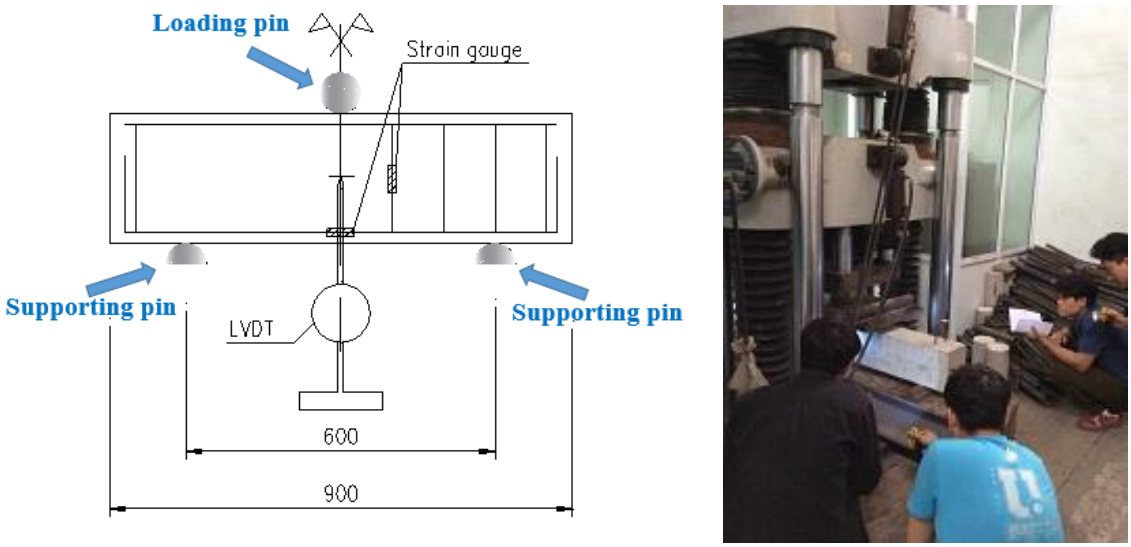

Figure 9. Schematization of 3-point bending test setup.

The ratio between the lever arm and the effective height of the section a/d equal to 1.35, corresponding to the case of short beam mentioned by U. Farooq et al[19]. The loading device is a hydraulic press of 300-ton capacity with a loading speed of 0.01 mm/s. The mid-span displacement measuring device is attached at the central position. The test is performed until apparition a fall of load and the concrete completely damaged. The values of force, mid-span displacement and deformation of the reinforcement were continuously monitored during the experiment. The cracks patterns are marked on both sides of the beam with a highlighter and the load corresponding to the moment of crack appearance is noted.

5. RESULTS AND DISCUSSIONS

5.1. Mode of failure and bearing behaviour

The failure modes of the beams are described in Figure 10, Figure 11 and Figure 12 respectively. Observing the test specimens, during the loading process, the first bending cracks appeared in the middle of the beam span. These cracks were continuing to extend and propagate while the load was increasing. The first shear cracks appeared in the middle of the beam, close to the position of the loading pin. Then, more inclined cracks were observed between the loading and the supporting pins. At maximal applying load corresponding to ultimate state, a diagonal major crack located in a haft of non-reinforced span, relying the loading and the supporting pins was notified. Simultaneously, the development of cracks adjacent to the bottom reinforcement along the lower layer towards the haft of non-reinforced span due to bond bursting.

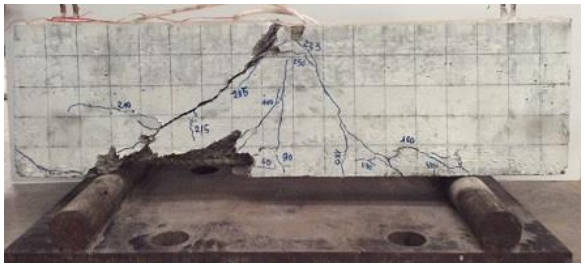

Figure 10. Failure pattern on specimen OSCB-S-0 without crushed oyster shells.

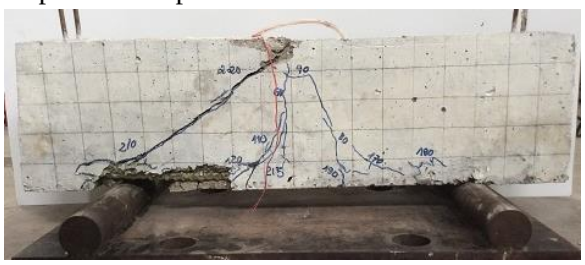

Figure 11. Failure pattern on specimen OSCB-S-25 with 25% natural sand volume replaced.by crushed oyster shells

Figure 12. Failure pattern on specimen OSCB-S-50 with 50% natural sand volume replaced.by crushed oyster shells.

This phenomenon is most clearly observed on beams OSCB-S-0 and OSCB-S-25. These beams are damaged when shear cracks develop and connect into inclined cracks from the loading pin to the supporting pins. In the proximity to the supporting pin on the non-reinforced side, the concrete surrounding the longitudinal reinforcement is heavily deteriorated. Otherwise, this did not happen on OSCB-S-50 specimen, showing that the presence of oyster shell increases the flexibility and bond properties of concrete. The cracks are denser and finer than those of OSCB-S-0 and OSCB-S-25 beams. Considering OSCB-S-25, the crack and failure distribution looks like a transition between shear-compression and diagonal-tension. This argument is consistent with the above analysis, therein the impact of crushed oyster shells on the flexibility and bond characteristic to the GFRP reinforcement is proved. The load-displacement relationship of the three beams is summarized on the graph in Figure 13. It was found that cracks in oyster concrete beams appear early from a smaller load level. This is due to the decrease of tensile flexural strength. When the destructive load is reached, damage occurs suddenly. In the present study, all the beams have high reinforcement content, leading to the main damage occurring on the concrete. This comes from the fact that GFRP reinforcement only works in the elastic domain, without plastic behaviour, leading to sudden and brittle failure.

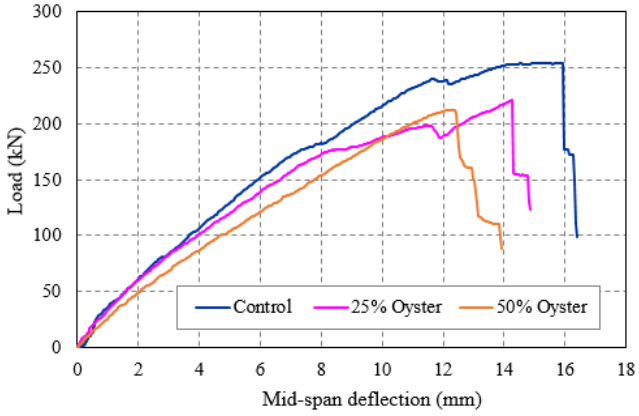

Figure 13. Load-deflection relationship at three kinds of specimens.

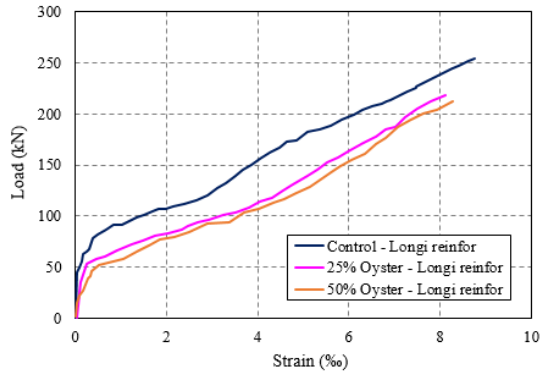

Figure 14. Load-strain relationship of longitudinal reinforcements at three kinds of specimens.

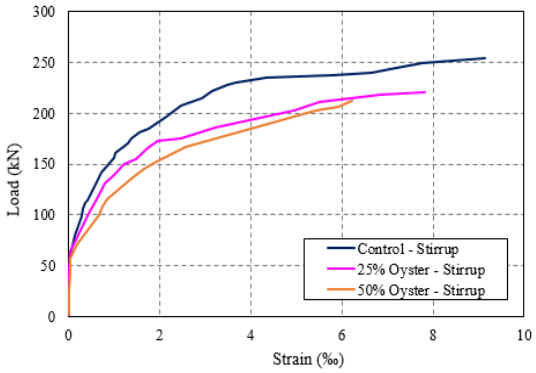

Figure 15. Load-strain relationship of stirrups at three kinds of specimens.

It is important to highlight that under the effect of the same load value, the control beam has less mid-span deflection than those of oyster concrete beams, resulting in less deformation of the tensile longitudinal reinforcement. Besides, the ultimate load of the OSCB-S-0 beam is also larger than the two beams OSCB-S-25 and OSCB-S-50, causing the stirrup of the OSCB-S-0 beam to also deform much and more obvious. The load-strain relationship of longitudinal and stirrup reinforcement is shown in Figure 14 and Figure 15. Depending on loading speed, the load-strain response of reinforcement could be classified in two or three main steps. The first one correspond to linear behaviour of structure, until the appearance of first crack in concrete. After that, it appears the load transferring from concrete to reinforcement, reflected eventually by a jump of strain under invariant load. In the third step, the failure pattern develops gradually until ultimate state, leading to a nonlinear load-strain relationship.

5.2. Prediction of shear strength by specifications and experimental results

It is noticed that the control beam has better shear resistance than those of the beam specimens containing 25% and 50% replacement oyster shells: The control beam OSCB-S-0 has a maximum shear resistance at 127.14kN, OSCB-S-25 specimen at 110.37kN and the OSCB-S-50 specimen at 105.92kN respectively. This argument is explained by the difference in mechanical properties of control concrete compared to oyster concrete. The critic values of

shear force (Vcr) causing first failure and ultimate shear resistance (Vu) are summarized in Table 4.

Table 4. Critic values of shear force causing failure and ratio Vcr/Vu at 3 beam specimens.

Categories	Pcr(kN)	Vcr(kN)	Pu(kN)	Vu(kN)	Vcr/Vu
OSCB-S-0	82.22	41.11	254.28	127.14	32%
OSCB-S-25	60.72	30.36	220.75	110.37	28%
OSCB-S-50	57.93	28.97	211.84	105.92	27%

In most cases, the shear strength achieved from experiment dominate those of theoretical provisions. Considering the results obtained by theories and experiments, it seems that the calculation by ACI 440.1R-15 specification is closer to the experimental results while those of JSCE 1997 specification is more towards safety. The two codes CSA S806-12 and BS-8110 given quite similar results, shown in Figure 16.

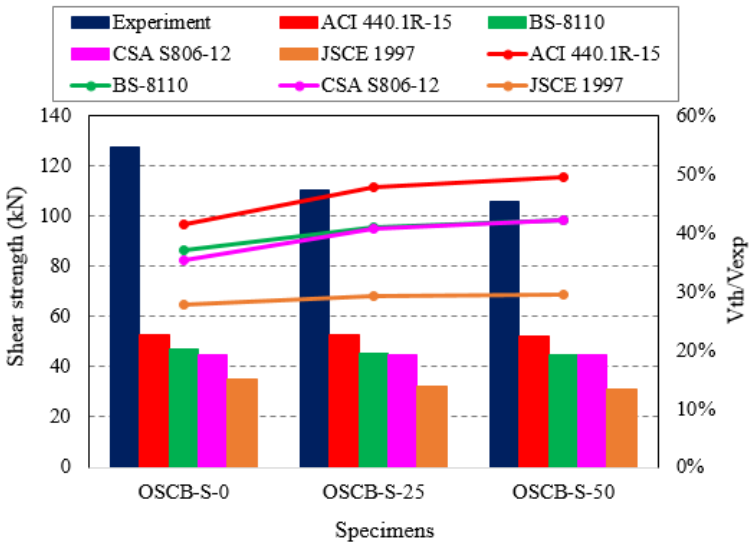

Figure 16. Comparing the shear strength of the haft span reinforced by different theoretical predictions and the experimental results.

Overall, the calculation results of the specifications are underestimated towards the safety (vary from 28% to 49%). Particularly, JSCE 1997 specification given the shear resistance of stirrups quite low, at only 47-49% compared to the shear resistance of concrete. This proportion in BS-8110 specification is 86-96% respectively. ACI 440.1R-15 code increases this ratio from 2.2 to 2.4 times and especially CSA S806-12 code has increased this ratio the most. The shear resistance of stirrups is 3.15 to 3.6 times bigger than those of concrete. Otherwise, compared to steel reinforcement, CSA S806-12 code predicts the shear resistance of FRP stirrups to be only 40% the one of concrete. This act due to the elastic modulus of FRP being much lower than that of traditional steel, significantly reducing the shear resistance of the stirrups.

6. CONCLUSION

In parallel with determining the mechanical properties of oyster shell concrete respectively in two cases 25% and 50% fine aggregate replaced, the beam specimens were cast and cured for 28 days before performing the experiment. In order to obtain the shear compression failure, the a/d is taken equal 1.35 for each beam. The experimental results

shown that the critic load also ultimate load of oyster shell concrete beams is lower than those of control concrete beams. Adding the ratio of oyster shell replacing the volume of natural sand raises the flexibility itself and bond properties to GFRP rebar is also improved, clearly shown in the 3-point bending test. The oyster shell concrete beams have lower bearing capacity and also shear strength. The failure pattern appears with greater density and smaller opening compared to the control beam. Many standard theoretical provision models for predicting shear strength have been carried out to refer to experimental results. The results given by the design standards are quite similar, tending to be safer than those of experiments.

ACKNOWLEDGMENT

This research is funded by University of Transport and Communications (UTC) under grant number T2023-XD-002TD.

REFERENCES

[1]. Vietnam Seafood Journal, Accelerating Krill Seed Production. https://thuysanvietnam.com.vn/tang-toc-san-xuat-giong-nhuyen-the/, (accessed 25 March 2024) (in Vietnamese.

[2]. Vietnam Family Newspaper, Does Bim Group's oyster processing factory handle the wastewater problem well? https://giadinhvietnam.com/nha-may-che-bien-hau-cua-bim-group-co-xu-ly-tot-van-de-nuoc-thai-d146406.html/, (accessed 25 March 2024). (in Vietnamese).

[3]. D. P. Steven, B.B. Dieter, K-P. Kunal, M Admir, J. B. Markus, B. Oral, Roadmap across the mesoscale for durable and sustainable cement paste – A bioinspired approach, Construction and Building Materials, 115 (2016) 13–31. https://doi.org/10.1016/j.conbuildmat.2016.04.020

[4]. J.P. Morris, Report synthesising the existing and potential uses of shells as by-products of the aquaculture industry, WP6: Mollusc shell production as a model for sustainable biominerals, 2017, Brussels, Belgium.

[5]. K.H. Mo, U.J. Alengaram, M.Z. Jumaat, S.C. Lee, W.I. Goh, C.W. Yuen, Recycling of seashell waste in concrete: A review, Construction and Building Materials, 162 (2018) 751–764. https://doi.org/10.1016/j.conbuildmat.2017.12.009

[6]. E.-I. Yang, M.-Y. Kim, H.-G. Park, S.-T. Yi, Effect of partial replacement of sand with dry oyster shell on the long-term performance of concrete, Construction & Building Materials, 24 (2010) 758–765.

[7]. O. Monita, A.M. Annisa, D. Lita, Mechanical properties of seashell concrete, Procedia Engineering, 125 (2015) 760-764.

[8]. S.A. Imad, Strut-and-tie model and its applications in reinforced concrete deep beams: A comprehensive review, Case Studies in Construction Materials, 19 (2023), https://doi.org/10.1016/j.cscm.2023.e02643.

[9]. F.J. Vecchio, M.P. Collins, Modified compression-field theory for RC elements subjected to shear, ACI Journal, (1986) 03-04.

[10]. ACI 440.1R-15, Guide for the Design and Construction of Structural Concrete Reinforced with Fiber-Reinforced Polymer Bars, 2015.

[11]. JSCE 1997, Code FRP Concrete Structures Using Continuous Fiber Reinforcing, 1997.

[12]. CSA S806-12, Design and construction of building structures with fibre-reinforced polymers, 2012.

[13]. BS 8110-1997, Structural Use of Concrete, 1997.

[14]. ACI 211.4R-08, Guide for Selecting Proportions for High-Strength Concrete Using Portland Cement and Other Cementitious Materials, 2008.

[15]. ASTM C39/C39M-17b, Standard Test Method for Compressive Strength of Cylindrical Concrete Specimens, 2017.

[16].ASTM C469–02, Standard Test Method for Static Modulus of Elasticity and Poisson's Ratio of

Concrete in Compression, 2002.
[17]. ASTM C78–02, Standard Test Method for Flexural Strength of Concrete (Using Simple Beam with Third-Point Loading), 2002.
[18]. ACI 318-14, Building Code Requirements for Structural Concrete and Commentary, 2014.
[19]. U. Farooq, K. Bedi, Study of Shear Behavior of RC Beams: Non Linear Analysis, Engineering Materials Science, Bloomsbury Publishing India Pvt Ltd., 2015, 3477-3488.

ANNEX
TYPICAL DESIGN CODES RELATED TO PREDICTION OF SHEAR PERFORMANCE

1. Guidelines by ACI 440.1R-15

Based on the formula of ACI 318 specification, according to ACI 440.1R-15, the shear capacity of concrete in FRP reinforced concrete structures is calculated as following:

$$V_c = \frac{2}{5} k \sqrt{f_c^{'}} b_w d \tag{1}$$

In which $f_c^{'}$ is the compressive strength of concrete (MPa), b_w is the width of the section (mm), d is the effective height of the beam (mm), k is the coefficient that takes account into the difference between traditional steel reinforcement versus FRP rebar in shear bearing of concrete beams. The coefficient k is calculated according to the following formula:

$$k = \sqrt{2\rho_f n_f + \left(\rho_f n_f\right)^2} - \rho_f n_f \tag{2}$$

Where ρ_f, n_f are respectively the percentage of FRP bar and the ratio of the elastic modulus of the FRP bar to the elastic modulus of the concrete. The shear resistance of stirrups is calculated similarly to that of stirrups in ACI 318 specification:

$$V_f = \frac{A_f f_{fv} d}{s} \tag{3}$$

In which A_f is the stirrup area, s is the distance between stirrup, f_{fv} is the controlled tensile strength of the stirrup to control the width of the shear crack and prevent the curved part of the stirrup being destroyed, calculated.by the following formula:

$$f_{fv} = 0,004 E_f \le f_{fb} \tag{4}$$

Where E_f and f_{fb} are the elastic modulus and bending strength of the FRP stirrup, respectively, determined based on the curved radius of the stirrup r_b, stirrup diameter d_b and tensile strength of the FRP stirrup f_{fu}:

$$f_{fb} = \left(0,05.\frac{r_b}{d_b} + 0,3\right).f_{fu} \le f_{fu} \tag{5}$$

Experimental researches show that the specimens having ratio r_b / d_b = 0, the bars will be deteriorated by shear at the curved position at very low loads. Therefore, the ratio r_b / d_b minimum should be equal to 3. In addition, the FRP belt must be closed with hooks with a 90° bend angle.

2. Guidelines by JSCE 1997

The first design recommendations and standards for concrete structures incorporating composite materials were published by the Japanese Society of Engineers in 1997 - JSCE Standard 1997[87], which stipulates that the resistance The shear of FRP reinforced concrete beams is determined basing on the same principles as traditional steel reinforcement. Accordingly, the shear strength of concrete beams is determined to be similar to the shear strength of concrete in reinforced concrete structures, incorporating an additional stiffness conversion coefficient between steel and FRP bars:

$$V_{cf} = 0,2\sqrt[4]{\frac{1}{d}}\sqrt[3]{100\frac{A_f}{b_w d}\frac{E_f}{E_s}}\sqrt[3]{f_c^{'}}b_w d \quad (6)$$

Where E_s is the elastic modulus of steel, E_f is the elastic modulus of FRP material. For ease of comparison with other calculation standards, formula (6) can be reduced to the following coefficients:

$$V_{cf} = \beta_d \beta_p 0,2\sqrt[3]{f_c^{'}}b_w d \quad (7)$$

Where $\beta_d = \sqrt[4]{\frac{1}{d}} \le 1,5$ (d in m) is the influence coefficient of size effect,

$\beta_d = \sqrt[3]{100\frac{A_f}{b_w d}\frac{E_f}{E_s}} \le 1,5$ is the influence coefficient of material.

Besides, the product $0,2.\left(f_c^{'}\right)^{1/3}$ ($f_c^{'}$ calculated in MPa) is also controlled not to exceed 0.72. The shear strength of FRP stirrups is also calculated based on the formula of traditional steel stirrups:

$$V_{sf} = \frac{A_{fw}E_{fw}\varepsilon_{fwd}}{s} z \quad (8)$$

Where A_{fw} is the stirrup area, E_{fw} is the elastic modulus of the FRP stirrup, and is the design deformation, determined by the following formula:

$$\varepsilon_{fwd} = \sqrt{\left(\frac{h}{0,3}\right)^{-1/10} f_c^{'}\frac{\rho_f E_f}{\rho_{fw}E_{fw}}10^{-4}} \quad (9)$$

Where ρ_f , ρ_{fw} are the ratio of longitudinal and stirrup reinforcement in the section, respectively. If the design stress $E_{fw}\varepsilon_{fwd}$ is greater than the strength of the bent area of the FRP stirrup f_{fb}, then this strength will be applied instead of the design stress $E_{fw}\varepsilon_{fwd}$. Then the strength of the bent FRP stirrup area is calculated according to the formula (5).

The way to calculate shear strength according to the JSCE Standard is quite similar to the ACI Standard: both use the deformability approach with the assumption that the strain and internal force in the FRP bar reinforcement are equal to deformation in steel reinforcement.

3. Guidelines by CSA S806-12

Similar to ACI 440.1R standard, CSA S806-12 standard [86] also stipulates the shear resistance of FRP reinforced concrete beams V_r based on the total shear resistance of concrete V_c and FRP stirrups V_f . The shear resistance of concrete is calculated according to the formula:

$$V_c = 0,05\lambda\phi_c k_m k_r k_a k_s \left(f_c^{'}\right)^{1/3} b_w d_v \tag{10}$$

In which λ is the density coefficient of concrete (=1 for normal concrete according to CSA S806-12, section 8.3.2.8), ϕ_c is the concrete resistance coefficient (=0.65 according to CSA S806-12, section 6.5.3.2), d_v is the effective height of the beam. The coefficients k_m, k_r , respectively the ratio of moment to shear force and the stiffness coefficient of longitudinal reinforcement, are calculated as follows:

$$k_m = \sqrt{\frac{V_f d}{M_f}} \tag{11}$$

$$k_r = 1 + \left(E_f \rho_f\right)^{1/3} \tag{12}$$

Where M_f and V_f are the bending moment and shear force at the calculated section. In case the calculated cross-section is located within a range of less than or equal to 2,5 d from the support, it is necessary to add the influence of the arch coefficient acting on the member, determined by the following formula:

$$1 \le k_a = 2,5\frac{V_f d}{M_f} \le 2,5 \tag{13}$$

In addition, for structures with effective shear height greater than 300 mm and shear stirrup content less than the minimum content, it is necessary to add a size influence factor when determining shear strength. of components:

$$k_s = \frac{750}{450 + d} \le 1 \text{ when } d > 300 \text{ mm} \tag{14}$$

The minimum stirrup content is determined according to the following formula:

$$A_{fv,\min} = 0,07\sqrt{f_c^{'}}\frac{b_w s}{0,4 f_{fu}} \tag{15}$$

The ratio between moment and shear force is calculated depending on the load-bearing diagram of the structure. Here in the 3-point bending diagram, this ratio is determined according to the formula $\frac{M}{V} = c$ where c is the distance from the support to the calculated cross-sectional position.

The above calculation formula V_c cannot be larger $0,22\phi_c\sqrt{f_c^{'}}b_w d_v$ and cannot be smaller $0,11\phi_c\sqrt{f_c^{'}}b_w d_v$ The shear resistance of FRP stirrups is calculated according to the following formula:

$$V_{sf} = \frac{0,4.\phi_f A_{fv} f_{fv} d_v}{s}\cot\theta \tag{16}$$

Where ϕ_f is the strength coefficient of the FRP stirrup, f_{fv} is the design tensile capacity of the FRP stirrup, the inclination angle of the compressive stress in concrete is calculated according to the formula $\theta = 30^{\circ} + 7000\varepsilon_1$, and is the average longitudinal strain at the point between calculated cross-sections:

$$\varepsilon_1 = \frac{\frac{M_f}{d_v} + V_f + 0,5N_f}{2E_f A_f} \tag{17}$$

In which, M_f, V_f, N_f are the bending moment, shear force and longitudinal force at the calculated section, respectively. For the 3-point bending test diagram in this thesis, you can see the longitudinal force at the calculated cross section $N_f = 0$.

4. Guidelines by BS-8110

BS-8110 standard determines the shear resistance of concrete in FRP reinforced concrete structures according to the following formula:

$$V_c = \frac{0,79}{\gamma_{me}}\left(\frac{100.A_{ref}}{b_w d_v}\frac{f_c^{'}}{25}\right)^{1/3}\left(\frac{400}{d}\right)^{1/4} b_w d_v \quad \text{when } \frac{a}{d} > 2,5 \tag{18}$$

$$V_c = \frac{0,79}{\gamma_{me}}\left(\frac{100.A_{ref}}{b_w d_v}\frac{f_c^{'}}{25}\right)^{1/3}\left(\frac{400}{d}\right)^{1/4} b_w d_v\left(2\frac{d_v}{a}\right) \text{ when } \frac{a}{d} < 2,5 \tag{19}$$

Where: $A_{ref} = \frac{A_r E_r}{200000}\gamma_{me}$

E_r - Elastic modulus of load-bearing reinforcement, not exceeding 200,000 MPa, γ_{me} - Elastic modulus coefficient, depending on FRP material, for GFRP γ_{me} = 1.8.

With the allowable limit deformation determined to be 0.25%, the shear strength of the stirrup is determined by the formula:

$$V_{sf} = \frac{0.0025E_{fw}A_{fw}}{\gamma_{me}}\frac{d}{s} \tag{20}$$